**Proceedings of the ASME 2011 International Design Engineering Technical Conferences &
Computers and Information in Engineering Conference
IDETC/CIE 2011
August 28-31, 2011, Washington, DC, USA**

DETC2011-47727

ON THE IDENTIFICATION OF MACHINE SETTINGS FOR GEAR SURFACE TOPOGRAPHY CORRECTIONS

Marco Gabiccini*
Dipartimento di Ingegneria Meccanica,
Nucleare e della Produzione
Università di Pisa
Largo Lucio Lazzarino 1, 56122 Pisa, Italy
Email: m.gabiccini@ing.unipi.it

Alessio Artoni
Massimo Guiggiani
Dipartimento di Ingegneria Meccanica,
Nucleare e della Produzione
Università di Pisa
Largo Lucio Lazzarino 1, 56122 Pisa, Italy

ABSTRACT

In this paper we set out to investigate the performances of some of the algorithms proposed in the gear literature for identifying the machine-settings required to obtain predesigned gear tooth surface topographies, or needed to compensate for flank form deviations of real teeth. For the ease of comparison, the problem is formulated as a nonlinear least-squares minimization, and the most widely employed algorithms are derived as particular cases. The algorithms included in the analysis are: (i) one-step methods; (ii) iterative methods; (iii) iterative methods with step control. The performance index is devised in their ability of returning practical solutions in the presence of: (i) strong model nonlinearities, (ii) ill-conditioning of the sensitivity matrix, (iii) demanding topographic shapes purposely selected. Instrumental here is an original classification of topographic modifications as either "simple" or "complex", based on the SVD analysis of the sensitivity matrix. On the basis of the numerical tests documented, iterative techniques with step control seem the most convenient, due to reliability and robustness of the solutions produced. The generation process here considered is face-milling of hypoid gears, even though the methodology is general enough to cope with any gear cutting method requiring only some minor technical changes.

INTRODUCTION

Most of the literature on machine setting identification stems from the necessity of minimizing the errors between the actual surface (inspected by CMMs[1]) and the theoretical one. However, the translation of the so-called *ease-off topography*, which optimally modifies the tooth surface *microgeometry*, into the corresponding machine-tool setting variations, leads to the very same problem. Therefore, this issue is a fundamental one in gear design and optimization, and has captured the attention of both industrial and academic researchers for the last 25 years.

Despite being such an active research area, the approaches proposed to tackle the problem are quite few, with some repetitions and, in the authors' opinion, with some of the methods actually lacking the necessary theoretical underpinnings. From a numerical optimization perspective, these approaches can be grouped into three main categories: (i) one-step methods, where *linear regression* (LR) analysis is applied, (ii) iterative methods, where linear regression analysis is *iteratively* applied (LRI), and (iii) iterative methods with step control, which actually embody numerical techniques for nonlinear optimization well established in other fields.

Representatives of group (i) are: [1, 2], where the error surface is approximated as a quadratic one, and the correction of first and second order terms is performed in two subsequent stages; [3], where the subroutine `DLSQRR` of IMSL Math/Library [4] is employed to solve the LR problem; [5–8], where the ill-conditioning of the sensitivity matrix is reported, and the singular value decomposition (SVD) is suggested as a mean to avoid numerical divergence; [9], where it is showed that near dependencies among machine parameters call for suitable regularization techniques [10] in the LR scheme, in order to produce meaningful solutions.

In group (ii) the following contributions can be counted: [11], where the Surface Match algorithm is proposed. Here, five *average* surface errors are defined and minimized by eventually solving a nonlinear system of five equations in five unknown ma-

*Address all correspondence to this author.
[1]Computer Measuring Machines.

chine settings. In [12, 13], a closed-loop correction process is presented, which is based on the iterative application of linear regression (LRI). Here, two variants of the method are proposed: in the first, the residual vector is the physical distance between mismatched points, while in the second the residual is represented by the coefficients of a polynomial interpolating the error surface. However, motivations for the choice of either the first or the second version seem to be lacking. Moreover, in terms of numerical efficiency, direct application of the definitions in Eqn. (21) and (22) in [12], or Eqn. (23) and (24) in [13], seems not advisable.

Group (iii) is comprised of contributions [14], [15], and [16]. In [14], the minimization of the real tooth surface deviations is framed as a *nonlinear minimization problem* for the first time. A cost function defined as the sum of the squared deviations is considered, and the IMSL subroutine `UMINF` in [4], implementing a quasi-Newton algorithm, is employed for the solution. In [15], the multifunctional optimization system tool (MOST), based on the sequential quadratic programming (SQP) method is used. Here, the cost function is defined as the maximum tooth surface deviation, and ill-conditioning is indirectly addressed by imposing bound constraints on the design variables.

Instead, in [16], the problem of identifying the machine settings, needed to generate a designed ease-off topography, is framed as a nonlinear least-squares problem and solved with the *Levenberg-Marquardt* method, with a trust-region approach. This choice allows to handle the ubiquitous ill-conditioning, arising from near dependencies between the machine parameters. This phenomenon becomes critical when a large number of them are selected as design variables, especially in combination with particular topographic "shapes".

In this paper, we present a comparison between three methods from groups (i), (ii), and (iii). For the ease of classification, machine settings identification is framed as a unique nonlinear minimization problem, and the investigated methods are derived as particular cases. The performance indices are devised in the ability of returning practical solutions, despite model nonlinearities and ill-conditioning, which seem intrinsic to the problem. Instrumental in evaluating the response to ill-conditioning is the SVD of the sensitivity matrix, which allows to classify topographic modifications as either "simple" or "complex".

PRELIMINARIES

Modern methods for computing spiral bevel and hypoid gear tooth flanks are based on mathematical models of their generating process. To cover all cases of generation, the various models of known gear-generating machine tools (e.g. Gleason, Hurth-Modul, Klingelnberg) can be generalized to a *virtual machine tool*, see for instance [17–19]. This idea of a virtual machine tool is commonly used by software that is designed for simulation, analysis and design of gear drives [20, 21]. Typically, a virtual machine tool incorporates approximately *sixty* design parameters to determine the geometry of the manufactured gear tooth flanks. For design parameters $\mathbf{x}$ (tool geometric parameters and coefficients of the polynomials controlling the machine joint functions [12]) fixed at given values $\bar{\mathbf{x}}$, we here consider the generated tooth surface as given by the following system

$$\mathbf{p}(\zeta,\bar{\mathbf{x}}), \text{ with } f(\zeta,\bar{\mathbf{x}})=0, \tag{1}$$

where $\zeta=(u,v,\varphi)$ collects the Gaussian and motion parameters [16], $\mathbf{p}(\zeta,\bar{\mathbf{x}})$ is the *enveloping family* of tool surfaces, and $f(\zeta,\bar{\mathbf{x}})=0$ is the *classical* equation of meshing [22, 23].

TOPOGRAPHY MODIFICATION

A vector $\mathbf{x}\in\mathbb{R}^n$ is defined that collects the n machine-tool settings selected as optimization variables. The symbol $\mathbf{x}_0$ denotes the values of the machine-tool settings of the basic design. The *basic* pinion tooth surface $\Gamma(\mathbf{x}_0)$ is sampled according to a two-dimensional grid of m points $\mathbf{p}_i^{(0)}$, $(i=1,\dots,m)$. Therefore, the initial grid on the basic tooth surface is uniquely represented by the coordinates of its points $\mathbf{p}_i^{(0)}$ and the components of its unit normals $\mathbf{n}_i^{(0)}$, where $\mathbf{p}_i^{(0)}:=\mathbf{p}(\zeta_i^{(0)},\mathbf{x}_0)$, and $\mathbf{n}_i^{(0)}:=\mathbf{n}(\zeta_i^{(0)},\mathbf{x}_0)$. The $\zeta_i^{(0)}$'s are the triplets associated with the i-th initial point, and $\mathbf{x}_0$ denotes the basic settings. As shown in Figure 1, the m target points $\mathbf{p}_i^*$ are defined by adding the predesigned ease-off values $h_i^{(0)}$ to the corresponding points along the initial unit normals, as follows

$$\mathbf{p}_i^* := \mathbf{p}_i^{(0)} + \mathbf{n}_i^{(0)} h_i^{(0)} \tag{2}$$

It is worth noting that the vector $\mathbf{h}_0=[h_1^{(0)}\cdots h_m^{(0)}]^T$ is referred to as *initial residual*, associated with the initial step $\mathbf{x}_0$, since it can be viewed as the *residual error* of the approximation of the target points with the basic ones.

The m point coordinates $\mathbf{p}_i^{(0)}$ are to be selected on both the active flank and the fillet of one side of the tooth if a single-side cutting method is adopted, or on both the concave and convex flanks, at the same time, if face-milling completing or face-hobbing processes are employed.

For generic values $\mathbf{x}$ of the machine-settings, with their associated tooth surface $\Gamma(\mathbf{x})$, the *residual* vector $\mathbf{h}(\mathbf{x})=[h_1(\mathbf{x})\cdots h_m(\mathbf{x})]^T$ and the corresponding triplets $\zeta_i(\mathbf{x})$'s can be obtained by solving the following nonlinear system of four scalar equations in the four scalar unknowns $\zeta_i\in\mathbb{R}^3$ and $h_i\in\mathbb{R}$

$$\begin{cases} \mathbf{F}_1 := \mathbf{p}_i^* - \mathbf{p}(\zeta_i,\mathbf{x}) - \mathbf{n}_i^{(0)} h_i = \mathbf{0} \\ F_2 := f(\zeta_i,\mathbf{x}) = 0, \end{cases} \tag{3}$$

where $\mathbf{F}_1\in\mathbb{R}^3$ and $F_2\in\mathbb{R}$. It is worth noting that, according to definition (3) (and differently from the one usually adopted [12, 16]), the generic residual $h_i(\mathbf{x})$ is computed along the *initial* normals $\mathbf{n}_i^{(0)}$. If on the one hand this choice allows to simplify the expressions in (3), and to reduce the computational cost (the quantities $\mathbf{n}_i^{(0)}$ are constant and computed only once), on the other it would call for a brief discussion of the existence and differentiability of the solutions of (3) as a function of the machine-settings $\mathbf{x}$, which is here omitted for brevity. The adoption of Eqn. (3) to define the residual h_i influences the definition of the Jacobian $\mathbf{J}$, which is a fundamental quantity in the later developments. It is worth recalling that $\mathbf{J}\in\mathbb{R}^{m\times n}$ is such that $J_{ij}=\partial h_i/\partial x_j$.

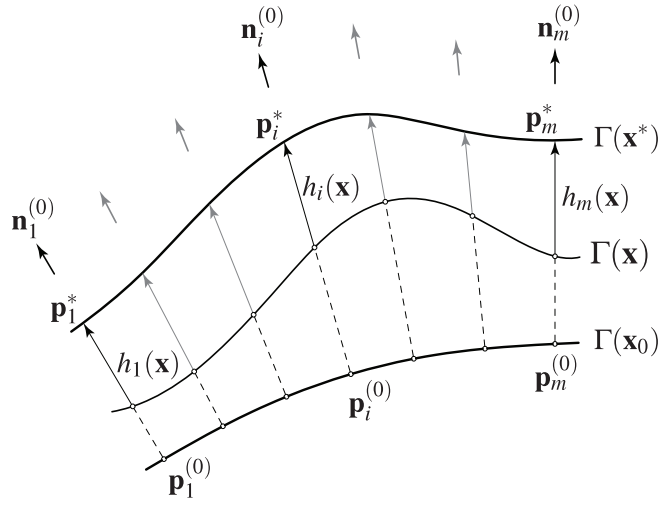

FIGURE 1. Residual $\mathbf{h}(\mathbf{x}) = [h_1(\mathbf{x}) \dots h_m(\mathbf{x})]^T$. $\mathbf{p}_i^{(0)}$: initial points on $\Gamma(\mathbf{x}_0)$; $\mathbf{p}_i^*$: target points on the target surface $\Gamma(\mathbf{x}^*)$; $\Gamma(\mathbf{x})$: surface with generic parameters $\mathbf{x}$.

IDENTIFICATION ALGORITHMS

To identify the unknown parameters $\mathbf{x}^*$, that is the machine settings required to generate the target surface ($\mathbf{p}_i^* = \mathbf{p}(\zeta_i^*, \mathbf{x}^*)$, with $i = (1, \dots, m)$, and for some ζ_i^*'s), a *minimization problem* can be set up with $\mathbf{x}$ as design variables, and where the objective is to minimize the residual (ideally, to make it zero). A possible approach is to define the following *nonlinear least-squares problem*

$$\mathbf{x}^* = \operatorname{argmin} f(\mathbf{x}), \quad f(\mathbf{x}) = \frac{1}{2}\mathbf{h}(\mathbf{x})^T\mathbf{h}(\mathbf{x}) \tag{4}$$

In this approach, the target machine-tool settings $\mathbf{x}^*$ will have the property of minimizing the measure of misfit (cost function $f(\mathbf{x})$) defined by the sum of the squared components of the residual.

The proposed framework is chosen since it lends itself to easily derive from it, as particular cases, the most widely used setting identification methods proposed in the gear literature. This helps in understanding what the methods ultimately aim at, and to unveil possible weak points. Let us now examine the three main categories into which such methods can be classified.

One-step methods

Let us build the second-order Taylor expansion $\bar{q}_k(\mathbf{s})$ of the objective function $f(\mathbf{x})$ in Eqn. (4) at the generic value $\mathbf{x}_k$ of the machine setting vector $\mathbf{x}$. Here, we introduced the correction vector $\mathbf{s} := \mathbf{x} - \mathbf{x}_k$. Explicitly, the quadratic model $\bar{q}_k(\mathbf{s})$ is given by

$$\bar{q}_k(\mathbf{s}) := f_k + \nabla f(\mathbf{x}_k)\mathbf{s} + \frac{1}{2}\mathbf{s}^T\nabla^2 f(\mathbf{x}_k)\mathbf{s}, \tag{5}$$

where the gradient $\nabla f(\mathbf{x}_k) \in \mathbb{R}^{1\times n}$ and the Hessian $\nabla^2 f(\mathbf{x}_k) \in \mathbb{R}^{n\times n}$ can be calculated by direct differentiation of f in (4) as

$$\nabla f(\mathbf{x}_k) = \mathbf{h}_k^T\mathbf{J}_k, \qquad \nabla^2 f(\mathbf{x}_k) = \frac{\partial}{\partial \mathbf{x}}\left(\mathbf{J}^T\mathbf{h}_k\right)\Big|_{\mathbf{x}_k} + \mathbf{J}_k^T\mathbf{J}_k \tag{6}$$

For conciseness, in Eqns. (5) and (6) the following positions were made $f_k := f(\mathbf{x}_k)$, $\mathbf{h}_k := \mathbf{h}(\mathbf{x}_k)$ and $\mathbf{J}_k := \mathbf{J}(\mathbf{x}_k)$. Usually, in nonlinear least-squares problems, the Hessian matrix $\nabla^2 f(\mathbf{x}_k)$ can be approximated by $\mathbf{H}_k := \mathbf{J}_k^T\mathbf{J}_k$ [24]. The resulting quadratic model $q_k(\mathbf{s})$ to be minimized is then

$$q_k(\mathbf{s}) := f_k + \mathbf{h}_k^T\mathbf{J}_k\mathbf{s} + \frac{1}{2}\mathbf{s}^T\mathbf{H}_k\mathbf{s} \tag{7}$$

To this end, we require that the partial derivative of $q_k(\mathbf{s})$ with respect to $\mathbf{s}$ be zero, thus obtaining

$$\mathbf{J}_k^T\mathbf{h}_k + \mathbf{H}_k\mathbf{s} = \mathbf{0} \tag{8}$$

or, by recalling that $\mathbf{H}_k = \mathbf{J}_k^T\mathbf{J}_k$, by *equivalently* writing

$$\mathbf{h}_k + \mathbf{J}_k\mathbf{s} = \mathbf{0} \tag{9}$$

Since $\mathbf{J}_k \in \mathbb{R}^{m\times n}$ in Eqn. (9) is usually a *tall* matrix, i.e. $m > n$ (the linear system is overdetermined), a possible approach is to use the *normal equations*, which stem naturally from the native version of the problem in Eqn. (8). By selecting this option one obtains the solution as

$$\mathbf{s}^{\mathrm{GN}} = -\mathbf{H}_k^{-1}\mathbf{J}_k^T\mathbf{h}_k = -\mathbf{J}_k^L\mathbf{h}_k, \quad \mathbf{J}_k^L := -(\mathbf{J}_k^T\mathbf{J}_k)^{-1}\mathbf{J}_k^T, \tag{10}$$

where $\mathbf{J}_k^L$ is the *left-inverse* of $\mathbf{J}_k$. However, it is worth recalling that $\mathbf{H}_k^{-1}$ (and hence $\mathbf{J}_k^L$) exists iff $\mathbf{J}_k$ is full column-rank (f.c.r.), and in general it is preferable to tackle directly Eqn. (9), e.g. via the SVD [25]. Despite the solution strategy eventually employed, the minimization step from Eqn. (10) is defined as *Gauss-Newton* step, and denoted by $\mathbf{s}^{\mathrm{GN}}$.

If we now consider we are building the quadratic model in the basic configuration, that is $k = 0$, and we are planning to find a solution in *one step* only, we end up with the following *linear regression* (LR) (equivalently, least-squares) problem

$$-\mathbf{J}_0\,\mathbf{s} = \mathbf{h}_0, \tag{11}$$

where $\mathbf{J}_0$ and $\mathbf{h}_0$ denote the Jacobian matrix and the residual vector calculated in the basic machine settings $\mathbf{x}_0$, respectively. It is worth noting that the vast majority of the works adopting this method (see, e.g., [3], [5], [6], [7], [12], [8], [13]) make use of the *sensitivity matrix* $\mathbf{S}_0$, where $\mathbf{S}_0 := -\mathbf{J}_0$.

It is worth also stressing that the very same problem is derived *equivalently* if the following *linear* approximation $\mathbf{h}_L$ of the residual is formed

$$\mathbf{h}(\mathbf{s}) \simeq \mathbf{h}_L(\mathbf{s}) := \mathbf{h}_0 + \mathbf{J}_0\,\mathbf{s} \tag{12}$$

and: either (a) the $\mathbf{h}_L(\mathbf{s})$ is zeroed, or (b) $\mathbf{h}_L(\mathbf{s})$ is substituted in Eqn. (4), and the *first* Gauss-Newton step in Eqn. (10) is adopted as the solution.

A fundamental aspect to stress is that the Jacobian $\mathbf{J}_k$ (as well as its initial version $\mathbf{J}_0$) is almost always an ill-conditioned matrix, i.e. its condition number is "high", and the naïve definition of $\mathbf{J}_k^L$ in Eqn. (10) leads to potentially meaningless numerical results. Ill-conditioning is caused by redundancy of the machine parameters, and it is worsened by increasing their number. Therefore, it is a ubiquitous problems when employing tool and kinematic parameters of all orders, i.e. in UMC-like machines [26].

The usual remedy to this situation, as proposed in [8], is to employ a *truncated* singular value decomposition (SVD), and/or apply some regularization method [10] directly to (the equivalent) problem in Eqn. (11). More insights into the possible effects caused by ill-conditioning of the Jacobian, and the difficulty of employing such techniques for restraining the solution norm will be discussed later.

Iterative methods

In iterative methods, the quadratic model $q_k(\mathbf{s})$ of the objective function $f(\mathbf{x})$ at the k-th step $\mathbf{x}_k$ is built as in Eqn. (7), and the sought minimum point $\mathbf{x}_{k+1}$ of $q_k(\mathbf{s})$ is used as the new starting point; the procedure is then repeated until some convergence criteria are met.

This perspective helps in clarifying that methods repeatedly solving Eqn. (9) with $k = 0, 1, \ldots$, that is LRI methods in group (ii) (for example iteratively calculating the steps by Eqn. (10)), are basically taking Gauss-Newton steps to minimize (7), *without* caring about their length. However, in the theory of numerical optimization the latter procedure is not even envisaged, since it is prone to instability, and better alternatives exist.

The iterative application of the Gauss-Newton step is proposed in [12] as a method to sequentially refine the machine-setting values, and it is defined as "closed-loop correction process". The main point here is that the hardware is "in the loop", and at each step the evaluation of the new residual entails: (i) the machining of a new gear set, and (ii) the CMM inspection of the generated flanks.

As a conclusion, it can be stated that systematic methods should be adopted to manage unfeasible solutions caused by ill-conditioning of the Jacobian, or by strong nonlinearities of the cost function f w.r.t. $\mathbf{x}$. Modern numerical methods exist that possess these features and are the subject of the next section.

Iterative methods with step control

The main idea behind iterative methods with step control strategies is that the quadratic model ought to be trusted only within a region were it represents f with sufficient accuracy. The quadratic model employed is always $q_k(\mathbf{s})$, for the following reasons: (i) the error in neglecting the first term in $\nabla^2 f(\mathbf{x}_k)$ of Eqn. (6) is acceptable if the residual is "small"– which tends to be increasingly true if a solution $\mathbf{x}^*$ exists such that $f(\mathbf{x}^*) = 0$, and the actual $\mathbf{x}_k$ is "approaching" to it – (ii) the computational cost is reduced since no additional derivative evaluations are required, (iii) with the approximation made, the Gauss-Newton step is always a descent direction for f, at least when $\mathbf{J}_k$ is full column rank and the gradient $\mathbf{h}_k^T\mathbf{J}$ is nonzero.

The first work applying these methods to machine-setting identification was published as early as 1991 by Litvin et al. [14]. Here, the quasi-Newton method implemented in the IMSL routine `UMINF` [4] was used. However, this choice does not allow to exploit the least-squares structure of the problem, nor the fact that the explicit expression of the gradient is available for the problem at hand (recall expression of $\nabla f(\mathbf{x}_k)$ in Eqn. (6)).

On the contrary, a method where the problem structure is fully exploited is [16]. Here, the Levenberg-Marquardt (LM) algorithm with a trust-region strategy is adopted. The minimization step $\mathbf{s}_k$ of the $k-$th quadratic approximation $q_k(\mathbf{s})$ in Eqn. (7) is restrained within a ball of radius Δ_k, that is

$$\mathbf{s}_k = \operatorname{argmin} q_k(\mathbf{s}), \;\; \text{with} \;\; \|\mathbf{s}\| \leq \Delta_k, \tag{13}$$

where Δ_k is adaptively modified in order to bound a region where the quadratic model $q_k(\mathbf{s})$ is *globally* descriptive of f. Different techniques can then be applied to solve the quadratic subproblem in Eqn. (13): the *dogleg method* is one of the most used. A detailed discussion of the implementation details of this particular technique for the machine-setting identification problem can be found in [16]. For a general discussion on numerical alternatives and convergence properties, [24] and [27] can be consulted.

In the rest of the paper, only the results obtained with the Levenberg-Marquardt algorithm described in [16] are presented. The motivation is that this implementation is very efficient, due to the profitable exploitation of the problem structure.

SOURCES OF NUMERICAL INSTABILITY

In this section we examine the main sources of numerical instability that may arise during the machine setting identification process. These are: (i) model nonlinearities, and (ii) ill-conditioning of the Jacobian matrix.

Model nonlinearities

The dependance of the cost function $f(\mathbf{x})$ in Eqn. (4) on the design variables $\mathbf{x}$ is *intrinsically nonlinear*, due to the involved trigonometric relationships between machine-tool settings and the corresponding topographic modifications. This aspect can be particularly critical when searching a solution by the linear regression (LR) method, or by iterative methods (LRI), if the necessary safeguards (essentially, a control of the step size) are not taken in due account.

Ill-conditioned Jacobian

Here we consider the issues that the algorithms have to face in the presence of an ill-conditioned Jacobian. The analysis is not limited to one-step methods only, since the solution of the linear problem in Eqn. (9) is also a basic ingredient of the iterative methods.

To simplify the notation, let us denote the Jacobian and the residual with the symbols $\mathbf{J}$ and $\mathbf{h}$, respectively. For the reader's convenience Eqn. (11) is here recalled

$$-\mathbf{J}\mathbf{s} = \mathbf{h} \tag{14}$$

The effect of ill-conditioning, i.e. the matrix condition number $\mathrm{K}(\mathbf{J})$ is a "big" number, is that "small" relative variations in the norm of $\mathbf{h}$ *may* cause "big" relative variations in the norm of the solution $\mathbf{s}$ (but it does not always happen). This is clearer by looking at the definition

$$\sup_{\delta\mathbf{h}\in D} \frac{\|\delta\mathbf{s}\|/\|\mathbf{s}\|}{\|\delta\mathbf{h}\|/\|\mathbf{h}\|} \leq \|\mathbf{J}\|\|\mathbf{J}^{-1}\| =: \mathrm{K}(\mathbf{J}), \tag{15}$$

where D is a set of possible values for the perturbations $\delta\mathbf{h}$. When the Euclidean norm is considered, the condition number can be calculated as $\mathrm{K}(\mathbf{J}) = \sigma_{\mathrm{M}}(\mathbf{J})/\sigma_{\mathrm{m}}(\mathbf{J})$, where $\sigma_{\mathrm{M}}(\mathbf{J})$ and $\sigma_{\mathrm{m}}(\mathbf{J})$ are the max and min singular values of $\mathbf{J}$. Culturally, ill-conditiong is usually coupled to the risk of instability of the solution $\mathbf{s}$ (e.g., caused by perturbations of the right-hand side $\mathbf{h}$, as in Eqn. (15)), which can occur as a consequence of truncation errors. Therefore, the usual mean to establish if the situation can be critical is to compare it to the machine precision ε: as a rule of thumb, $\varepsilon\,\mathrm{K}(\mathbf{J})$ represents the precision preserved in the representation of the solution. Note that in this context, the *shapes* of the truncation errors are never investigated.

Now we discuss some issues of ill-conditioning not directly related to the loss of precision of the solution, that are to be considered as the actual source of troubles when identifying the machine-setting corrections. For a complete understanding, a short detour into linear algebra is necessary.

The Jacobian matrix $\mathbf{J} \in \mathbb{R}^{m\times n}$, $m > n$, can be decomposed via the SVD [25] as follows

$$\mathbf{J} = \mathbf{U}\Sigma\mathbf{V}^T = \begin{bmatrix}\mathbf{R} & \mathbf{N}\end{bmatrix} \begin{bmatrix}\Sigma_n \\ \mathbf{0}\end{bmatrix} \mathbf{V}^T, \tag{16}$$

where we assumed, as it always happens in practice, that $\mathbf{J}$ is f.c.r. (i.e. $\mathrm{rank}(\mathbf{J}) = r = n$). $\Sigma_n = \mathrm{diag}(\sigma_1, \ldots, \sigma_n) \in \mathbb{R}^{n\times n}$, with $\sigma_1 \geq \sigma_2 \geq \cdots \geq \sigma_n > 0$. The n columns $\mathbf{R} \in \mathbb{R}^{m\times n}$, with $\mathbf{R} = [\mathbf{r}_1 \cdots \mathbf{r}_n]$, represent an orthogonal basis for $\mathscr{R}(\mathbf{J})$ (the range space of $\mathbf{J}$) in $\mathbb{R}^m$, while the $m-n$ columns $\mathbf{N} \in \mathbb{R}^{m\times(m-n)}$, with $\mathbf{N} = [\mathbf{n}_1 \cdots \mathbf{n}_{m-n}]$, form an orthogonal basis for $\mathscr{N}(\mathbf{J}^T)$ (the null space of $\mathbf{J}^T$). It is worth recalling that $\mathbb{R}^m$ is the space where the residuals $\mathbf{h}$ are defined.

Similarly, we can define an orthogonal decomposition of $\mathbb{R}^n$, which is the space where the solutions $\mathbf{s}$ are defined. However, since $\mathbf{J}$ is f.c.r., it does not admit a null space, i.e. $\mathscr{N}(\mathbf{J}) = \mathbf{0}$, and $\mathbb{R}^n = \mathscr{R}(\mathbf{J}^T)$. Therefore, this space is entirely spanned by the n columns of $\mathbf{V} \in \mathbb{R}^{n\times n}$, with $\mathbf{V} = [\mathbf{v}_1 \cdots \mathbf{v}_n]$.

Let us now look for a solution of Eqn. (14) via the SVD. By exploiting the orthogonality properties of $\mathbf{U}$ and $\mathbf{V}$, one writes

$$-\mathbf{U}\Sigma\mathbf{V}^T\mathbf{s} = \mathbf{h} \;\rightarrow\; -\Sigma\mathbf{V}^T\mathbf{s} = \mathbf{U}^T\mathbf{h} \tag{17}$$

If the positions $\bar{\mathbf{s}} := \mathbf{V}^T\mathbf{s}$ and $\bar{\mathbf{h}} := \mathbf{U}^T\mathbf{h}$ are made the solution obtained via the pseudoinverse of Σ is given by

$$\bar{\mathbf{s}} = -\Sigma^+\bar{\mathbf{h}} \iff \bar{\mathbf{s}} = -[\Sigma_n^{-1} \;\; \mathbf{0}]\bar{\mathbf{h}}, \tag{18}$$

where $\Sigma_n^{-1} = \mathrm{diag}(1/\sigma_1, \ldots, 1/\sigma_n)$. Therefore, in the new coordinates $\bar{\mathbf{s}}$ and $\bar{\mathbf{h}}$, the equations (14) are decoupled, and it is quite easy to "see" the effect of requiring a particular topographic modification on the least-squares solution. In fact, if $\bar{\mathbf{h}} = \mathbf{e}_1^m = [1\,0\cdots 0]^T \in \mathbb{R}^m$ (here $\mathbf{e}_p^q$ is the p-th element of the canonical basis in a space of dimension q), then the solution is $\bar{\mathbf{s}} = -(1/\sigma_1)\mathbf{e}_1^n = -[1/\sigma_1\, 0\cdots 0]^T \in \mathbb{R}^n$.

In the original coordinates, hence in terms of actual topography modifications and machine setting corrections, the unitary ease-off $\mathbf{h} = \mathbf{U}\mathbf{e}_1^m = \mathbf{u}_1$ calls for machine setting corrections $\mathbf{s} = -(1/\sigma_1)\mathbf{V}\mathbf{e}_1^n = -(1/\sigma_1)\mathbf{v}_1$. This is true for each $i \in (1, \ldots, n)$, and a variation of the residual along the i-th column $\mathbf{u}_i$ of $\mathbf{U}$ calls for a correction of the machine-settings along the i-th column $\mathbf{v}_i$ of $\mathbf{V}$, properly scaled by the reciprocal of the associated singular value. Adapting the general definitions [25] to the problem at hand, the columns $\mathbf{u}_i$ can be defined as *eigen-topographies*, while the scaled columns $-(1/\sigma_i)\mathbf{v}_i$ can be defined as *eigen-corrections*. Then, a principled way to distinguish between a "simple" or a "complex" eigen-topography can be devised according to the *length* of the required correction, which is strictly related to its practical applicability (the new settings must be acceptable to the machine and/or the underlying mathematical model must converge). Therefore, the first eigen-topography $\mathbf{h} = \mathbf{u}_1$ requires the eigen-correction $\mathbf{s} = -(1/\sigma_1)\mathbf{v}_1$, where usually $1/\sigma_1 \ll 1$, and has to be considered as the "simplest" one. On the contrary, the last eigen-topography $\mathbf{h} = \mathbf{u}_n$ has to be considered the most "complex" one, since it calls for the last eigen-correction $\mathbf{s} = -(1/\sigma_n)\mathbf{v}_n$, where usually $1/\sigma_n \gg 1$, which is likely to be of no practical use. As evident, the more the Jacobian is ill-conditioned, the more eigen-topographies associated to small singular values cause divergence in the solution.

As clearly evidenced by the SVD decomposition, $\mathscr{N}(\mathbf{J}^T)$ denotes that portion of $\mathbb{R}^m$ which is *unreachable* by the linear model, that is the space of the *unreachable* topographic modifications. Residuals belonging to $\mathscr{N}(\mathbf{J}^T)$ cannot be compensated at all, and the corresponding corrections are set to zero, that is $\mathbf{s} = \mathbf{0}$.

On the basis of the above considerations, it will be shown that ill-conditioning (which is always present when many parameters are considered) is critical when it is associated to "complex" topographic corrections (i.e., eigen-topographies of higher order, or their combinations).

With $\mathbf{x} = \mathbf{x}_0$ in Table 1, the topographic modifications $\mathbf{u}_i$ associated with the i-th singular value σ_i ($i = 1, \ldots, 20$), are depicted in Figure 2 in increasing order of "complexity". Quite interestingly, the columns $\mathbf{u}_1$ to $\mathbf{u}_3$ resemble first-order ease-off corrections, $\mathbf{u}_4$ to $\mathbf{u}_9$ recall second-order corrections, while $\mathbf{u}_i$ with $i \geq 10$ get increasingly wavy and progressively similar to random noise.

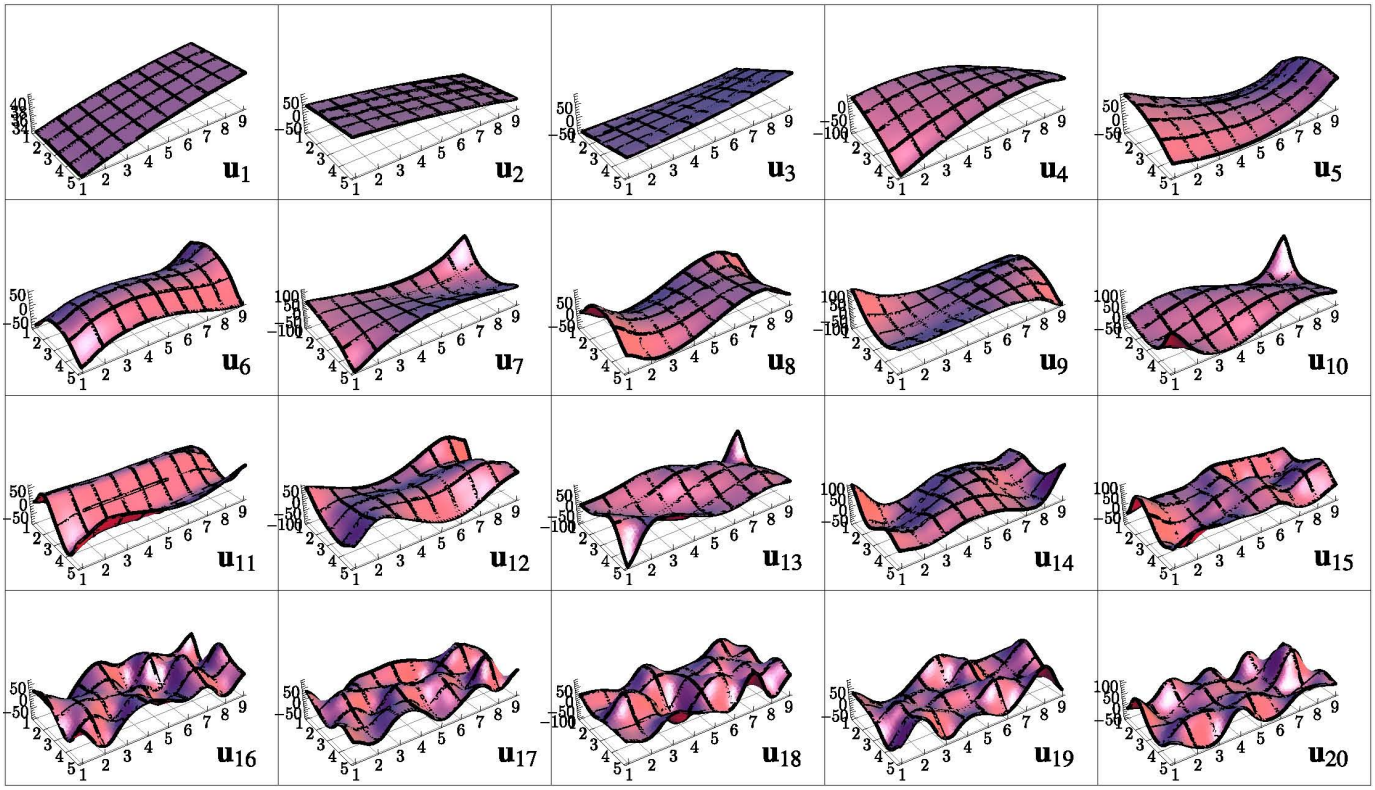

FIGURE 2. Eigen-topographies $\mathbf{u}_i$, with $(i = 1, \ldots, 20)$.

NUMERICAL TESTS

In this section a comparison of the three methods LR, LRI, and LM belonging to groups (i), (ii), and (iii), respectively, is presented. The performance index is devised in the ability of the methods to return practical solutions in the presence of: (i) model nonlinearities, (ii) ill-conditioning of the Jacobian matrix, when either "simple" or "complex" eigen-topographies have to be obtained. It worth observing that, in general, nonlinearities and ill-conditioning are usually coupled.

In the following numerical experiments, the tooth active flank is sampled according to a typical 9×5 grid (9 points lengthwise and 5 profilewise): therefore $\mathbf{h} \in \mathbb{R}^{45}$. The parameter types and their basic values are reported in the first two columns of Table 1.

Model nonlinearities

To highlight the effect of the sole nonlinearity, the following test is conceived. The spherical radius R_1 is assigned the new value $R_1^* = 150.00$ mm, and the corresponding ease-off $\bar{\mathbf{h}}$, associated with this modification, is computed with respect to the basic configuration (with $R_1^{(0)} = 350.897$ mm) in Table 1. Then, starting from the basic configuration $R_1^{(0)}$, and given $\bar{\mathbf{h}}$, the (un)known *global* minimum point R_1^* has to be identified by changing *only* R_1. In other words, the design variable is $\mathbf{x} = x = R_1 \in \mathbb{R}$, its initial value is $x_0 = 350.897$ mm, and the initial residual is $\bar{\mathbf{h}}$.

The results of the identification process by applying different methods are reported in Figure 3. As evident from this plot, the solution $x^{\mathrm{GN}} := x_0 + s^{\mathrm{GN}}$ returned by the linear regression method (i) (i.e., the minimum point of the quadratic approximation $q_0(s)$ of $f(x)$ around x_0, computed as in Eqn. (10)) is not satisfactory due to the highly non-quadratic behavior of the cost function $f(x)$ "far" from x_0. Since the value x^{GN} is not practicable, also the methods of type (ii) would fail, as they would re-start from an out-of-range setting.

On the contrary, iterative methods of type (iii), by wisely controlling the step length, return the solution $x_6 = x^*$, after just six iterations.

Ill-conditioning

In the tests that follow, we consider a design vector $\mathbf{x} \in \mathbb{R}^{20}$ which collects 20 variables chosen among tool geometric parameters and coefficients of the polynomial functions (up to the third order) that control the machine motions.

Simple ease-off topography. As the first test case, we identify the machine-settings needed to obtain the lengthwise crowning depicted in Figure 4. By virtue of the eigen-topography classification in Figure 2, this ease-off definitely rates among the "easy" ones. It has been defined by purposely perturbing R_p, S_0 and q_0 according to Stadtfeld's formulas (5.9) in [28], p.80. The residual $\mathbf{h}_0$ is computed according to the definition, with respect to the tooth geometry associated to $\mathbf{x}_0$. This choice guaran-

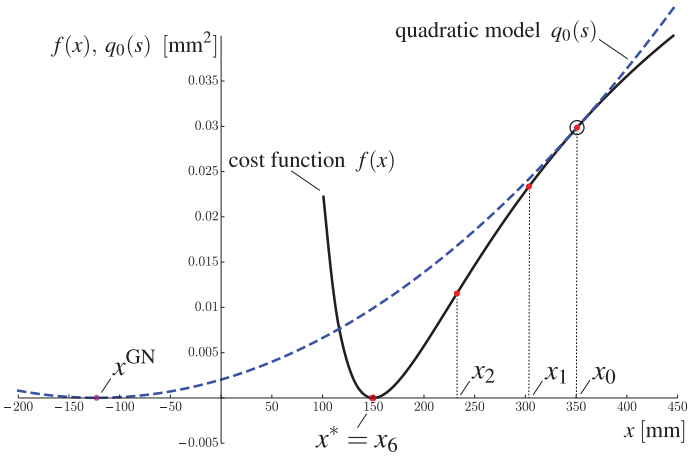

FIGURE 3. Effects of model nonlinearities on the solution. Black solid: nonlinear cost function $f(x)$; blue dashed: quadratic model $q_0(s)$; x^{GN} solution obtained by linear regression; $x_6 = x^*$ global solution obtained with iterative methods with step control.

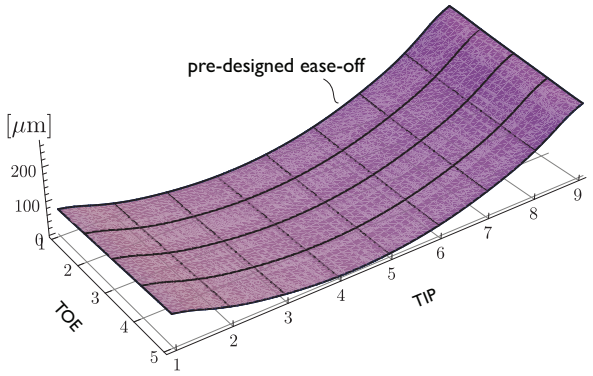

FIGURE 4. Lengthwise crowning defined by variation of R_p, S_0 and q_0 through Stadtfeld's formulas [28].

tees that a global solution $\mathbf{x}^* \in \mathbb{R}^{20}$ exists ($\mathbf{h}(\mathbf{x}^*) = \mathbf{0}$), is known, and can be used as a reference to properly assess the converge properties of the algorithms to be tested. The values of the predesigned corrections are $\Delta R_p = +5.01127$ mm, $\Delta S_0 = +2.23637$ mm, and $\Delta q_0 = +3.5083$ deg, and corresponding new values are $R_p^* = 84.0242$ mm, $S_0^* = 74.3764$ mm, and $q_o^* = 63.2453$ deg. It is worth remarking that the other parameters are kept fixed at their basic values, as shown in Table 1.

In the basic configuration $\mathbf{x}_0$, $\mathrm{K}(\mathbf{J}_0) = 1.8874 \cdot 10^8$. If we perform calculations with a machine epsilon $\varepsilon \simeq 10^{-16}$ (which is a standard value for double precision) we are guaranteed to preserve an accuracy of at least 8 digits when solving Eqn. (11)

PARAMETER	BASIC VALUE $\mathbf{x}_0$	KNOWN SOLUTION $\mathbf{x}^*$
Cutter point radius R_p (mm)	79.0130	84.0242
Spherical radius R_1 (mm)	350.8970	same
Blade angle α_p (deg)	17.4200	same
Radial setting S_0 (mm)	72.1400	74.3764
Blank offset E_0 (mm)	−5.0800	same
Sliding base B_0 (mm)	−1.5192	same
Cradle angle q_0 (deg)	59.7369	63.2453
Machine root angle γ_0 (deg)	33.6731	same
Ratio of roll m_0	1.7066	same
2C	0.0226	same
6D	−0.0329	same
24E	0.0000	same
120F	0.0000	same
Mach. center to back D_0 (mm)	2.7184	same
B_1 (mm/rad)	0.0000	same
B_2 (mm/rad^2)	0.0000	same
B_3 (mm/rad^3)	0.0000	same
E_1 (mm/rad)	0.0000	same
E_2 (mm/rad^2)	0.0000	same
E_3 (mm/rad^3)	0.0000	same

TABLE 1. Basic settings $\mathbf{x}_0$ and predefined global solution $\mathbf{x}^*$ used for the numerical tests.

by the SVD. Therefore, if the proper safeguards are taken, loss of precision due to ill-conditioning is not a critical issue here. However, since $\mathrm{K}(\mathbf{J}_0^T\mathbf{J}_0) = 3.5619 \cdot 10^{16}$, adopting the naïve method in Eqn. (10), with direct calculation of the left-inverse of $\mathbf{J}_0$, one faces the risk of getting meaningless results, since not a single significant digit may be correct in the solution.

Now we turn to iterative methods without step control. If we apply the algorithm suggested in [12], which is the iterative calculation and application of the Gauss-Newton step, we get the solutions reported in Table 2. Already at the fourth iteration $\mathbf{x}_4$ the residual $\mathbf{h}(\mathbf{x}_4)$ is very small and the overall result can be considered satisfactory. However, by looking at the evolution of the residual norm $\|\mathbf{h}(\mathbf{x}_i)\|$, with $(i = 0,\ldots,4)$, it can be argued that the method has been "lucky" to retrace its steps. In fact, after the first step, the direction taken was not a descending one (the residual norm increased and no safeguard was provided by the method): this fact, in other circumstances, may have caused divergence.

The solution returned by one-step methods would be $\mathbf{x}_1$ which is clearly a terrible choice (the residual increased).

If we employ the iterative method with step control based on a trust region strategy proposed in [16], we obtain the first four steps reported in Table 3. Here the residual norm $\|\mathbf{h}(\mathbf{x}_i)\|$ decreases apparently more slowly compared to the iterative method in Table 2: but, at least, it proceeds in a safe and predictable manner, since the decrease is monotonic. However, there is no reason to stop iterating just after a specified number of steps. In fact, if the iterations are repeated until reasonable convergence criteria are met (here 16 steps are needed), one ends up with the solution $\mathbf{x}_{16}$ in the last column of Table 3, which allows to identify *exactly* the predesigned topography (as confirmed by the residual norm value). The actual residual obtained is exactly overlapped to the pre-designed one, and its figure is omitted since it would be identical to Figure 4.

Incidentally, it is worth noting that the returned solution $\mathbf{x}_{16}$ is a global one (the residual is numerically zero), and it is distinct from $\mathbf{x}^*$. This means that the identification problem, at least for

PARAMETER	BASIC VALUE $\mathbf{x}_0$	1-ST STEP $\mathbf{x}_1$	2-ND STEP $\mathbf{x}_2$	3-RD STEP $\mathbf{x}_3$	4-TH STEP $\mathbf{x}_4$
Cutter point radius R_p (mm)	79.0130	83.1011	83.6974	83.68	83.7016
Spherical radius R_1 (mm)	350.8970	350.663	351.731	351.577	351.772
Blade angle α_p (deg)	17.4200	18.3686	17.5145	17.358	17.2803
Radial setting S_0 (mm)	72.1400	71.544	72.098	71.9588	72.1196
Blank offset E_0 (mm)	−5.0800	−6.85149	−6.66925	−6.69913	−6.55853
Sliding base B_0 (mm)	−1.5192	−2.40518	−1.37992	−1.17066	−1.15384
Cradle angle q_0 (deg)	59.7369	63.6728	64.0183	64.1896	64.2011
Machine root angle γ_0 (deg)	33.6731	34.6085	33.8799	33.7575	33.6957
Ratio of roll m_0	1.7066	1.65746	1.66576	1.66476	1.66859
2C	0.0226	0.0141076	0.0138691	0.0137685	0.012635
6D	−0.0329	0.0018602	−0.0284836	−0.0213934	−0.0289352
24E	0.0000	−0.00233724	0.0371361	−0.00591707	0.00185444
120F	0.0000	0.468629	−0.181301	0.0703083	−0.0830065
Mach. center to back D_0 (mm)	2.7184	0.0966167	0.365558	0.0945179	0.192392
B_1 (mm/rad)	0.0000	−1.56298	−0.349604	−0.128212	−0.03856
B_2 (mm/rad^2)	0.0000	2.99858	0.897106	0.0125777	−0.0667912
B_3 (mm/rad^3)	0.0000	−5.06704	−7.15252	−6.6867	−7.19538
E_1 (mm/rad)	0.0000	−0.819061	−1.09494	−1.33243	−1.34861
E_2 (mm/rad^2)	0.0000	−1.98245	−1.39852	−1.29431	−1.09975
E_3 (mm/rad^3)	0.0000	0.0953315	−0.560977	−0.0427466	−0.284481
RESIDUAL NORM $\|\mathbf{h}(\mathbf{x}_i)\|$	$709.566 \cdot 10^{-3}$	$\mathbf{816.299 \cdot 10^{-3}}$	$32.6796 \cdot 10^{-3}$	$0.5572 \cdot 10^{-3}$	$0.38313 \cdot 10^{-3}$

TABLE 2. Lengthwise crowning. Iterative method without step control: iterations and cost function.

PARAMETER	BASIC VALUE $\mathbf{x}_0$	1-ST STEP $\mathbf{x}_1$	2-ND STEP $\mathbf{x}_2$	3-RD STEP $\mathbf{x}_3$	4-TH STEP $\mathbf{x}_4$	SOLUTION ($\mathbf{x}_{16}$)
Cutter point radius R_p (mm)	79.0130	83.3295	83.4645	83.4893	83.4385	83.4415
Spherical radius R_1 (mm)	350.8970	349.803	349.624	349.678	349.627	349.645
Blade angle α_p (deg)	17.4200	18.51	17.58	17.10	17.04	17.03
Radial setting S_0 (mm)	72.1400	73.0076	73.2475	73.3533	73.4683	73.6778
Blank offset E_0 (mm)	−5.0800	−6.16832	−6.21415	−6.0840	−5.9888	−5.7866
Sliding base B_0 (mm)	−1.5192	−2.85704	−3.18557	−3.06747	−3.26836	−3.30598
Cradle angle q_0 (deg)	59.7369	62.7654	62.9805	63.1028	63.089	63.1203
Machine root angle γ_0 (deg)	33.6731	34.6319	34.0202	33.6714	33.648	33.6411
Ratio of roll m_0	1.7066	1.6765	1.67739	1.6809	1.68336	1.6887
2C	0.0226	0.02734	0.0332917	0.0319936	0.0322285	0.0304488
6D	−0.0329	0.008652	0.00833984	0.000554519	−0.00112532	−0.0116756
24E	0.0000	0.033772	0.013159	0.0187673	0.0173679	0.0242835
120F	0.0000	0.631915	0.638027	0.45208	0.438806	0.287625
Mach. center to back D_0 (mm)	2.7184	2.1616	2.33659	2.36549	2.45289	2.52707
B_1 (mm/rad)	0.0000	−1.61065	−0.557492	0.0211364	0.0552485	0.0532945
B_2 (mm/rad^2)	0.0000	3.4023	0.892103	0.322951	0.142047	−0.0005663
B_3 (mm/rad^3)	0.0000	−3.60877	−3.29018	−3.09186	−3.11647	−3.33488
E_1 (mm/rad)	0.0000	0.502459	0.365106	0.203197	0.22442	0.181836
E_2 (mm/rad^2)	0.0000	−1.84221	−1.58254	−1.39418	−1.27365	−0.972905
E_3 (mm/rad^3)	0.0000	2.05357	2.98662	2.46194	2.59446	2.1657
RESIDUAL NORM $\|\mathbf{h}(\mathbf{x}_i)\|$	$709.566 \cdot 10^{-3}$	$132.259 \cdot 10^{-3}$	$92.6702 \cdot 10^{-3}$	$12.7768 \cdot 10^{-3}$	$0.7655 \cdot 10^{-3}$	$4.31 \cdot 10^{-12}$

TABLE 3. Lengthwise crowning. Iterative method with step control: iterations and cost function.

such a large number of design variables, admits multiple global solutions.

Complex ease-off topography. As the second test case, we consider the problem of finding the machine-setting corrections to obtain the topographic modification $\bar{\mathbf{h}} = 0.25\,\mathbf{u}_{12}$. This is a scaled (reduced) version of the eigen-topography $\mathbf{u}_{12}$ of Figure 2, which is shown more clearly in Figure 5.

As previously noted, this topography is known to be quite unpleasant. In fact, it is associated to the "small" singular value $\sigma_{12} = 1.1552 \cdot 10^{-4}$, and it calls for a correction $\mathbf{s} = -(1/\sigma_{12})(0.25\mathbf{v}_{12})$, which may not be compatible with machine and tool physical limits. In more detail, the corrections for the design variables $\mathbf{x} \in \mathbb{R}^{20}$ obtained by one-step methods are reported in Table 4. It is easy to note that this solution is practically meaningless, since many of the suggested corrections are out of range. However, a policy based on the truncated SVD (the singular values below a certain threshold are omitted in the decomposition) is completely useless here, and would suggest a null correction. This because the effect of discarding the singular values below σ_{12} is to augment the null space of $\mathbf{J}_0^T$ by all the $\mathbf{u}_i$'s, with $i \geq 12$. This approach does not allow to move further in the identification process and it sounds like a surrender.

Note that the iterative methods without step control would face exactly the same problem, since they are not able to overcome the first step.

For such a complex task, also when considering the iterative methods with step control, we are faced with the unavoidable technological limitations. However, since these methods tackle the problem really as a nonlinear one, at least they are able to "move beyond" the linear approximation. As shown in Table 5, the iterative method with step control reduces the residual norm by 19%, already after six iterations. More importantly, also in this case the method is capable of managing the ill-conditioning with ease, returning a practical answer.

The designed and the obtained topographies are shown in Figure 6.

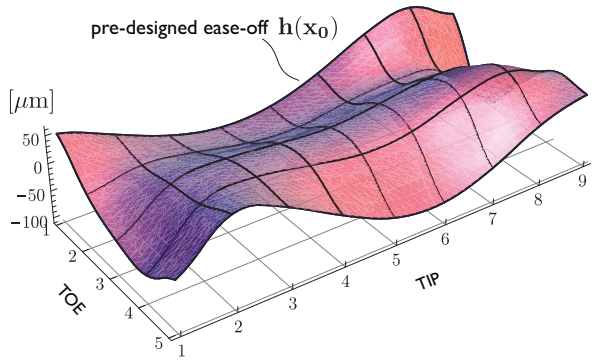

FIGURE 5. Complex ease-off. Modification proportional to the 12-th eigen-topography $\mathbf{u}_{12}$, i.e. $\mathbf{h}(\mathbf{x}_0) = 0.25\,\mathbf{u}_{12}$.

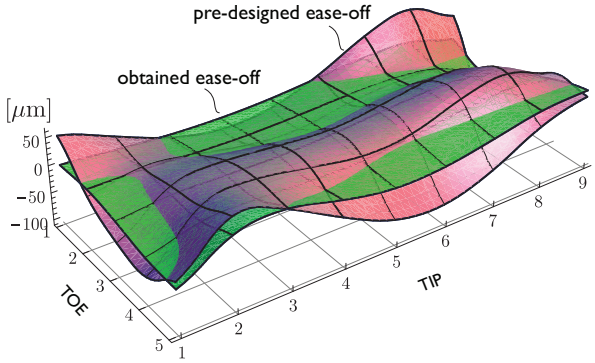

FIGURE 6. Complex ease-off. Predesigned and obtained topographies after six steps of the Levenberg-Marquardt algorithm [16]: iterative method with step control.

CONCLUSIONS

Some widely recognized but seldom investigated issues have been analyzed in detail. By accurately tailoring some numerical tests in which these obstacles come noticeably into play, the performances of some of the most popular algorithms for machine-setting identification have been assessed. Algorithms based on iterative approximations of the residual, where the step length is adaptively controlled, seem the most effective in returning practical and robust solutions. Therefore, as a final suggestion, the use of routines based on the Levenberg-Marquardt algorithm is certainly recommended for the solution of the identification problem.

PARAMETER	BASIC VALUE $\mathbf{x}_0$	SUGGESTED VARIATION $\mathbf{s}$
Cutter point radius R_p (mm)	79.0130	+170.898
Spherical radius R_1 (mm)	350.8970	−16.7091
Blade angle α_p (deg)	17.4200	+411.76
Radial setting S_0 (mm)	72.1400	−252.1
Blank offset E_0 (mm)	−5.0800	−640.058
Sliding base B_0 (mm)	−1.5192	−63.6513
Cradle angle q_0 (deg)	59.7369	−635.158
Machine root angle γ_0 (deg)	33.6731	+293.57
Ratio of roll m_0	1.7066	−13.9546
2C	0.0226	+21.1555
6D	−0.0329	−12.4575
24E	0.0000	+232.423
120F	0.0000	+179.569
Mach. center to back D_0 (mm)	2.7184	+581.482
B_1 (mm/rad)	0.0000	−801.452
B_2 (mm/rad^2)	0.0000	−1043.54
B_3 (mm/rad^3)	0.0000	−22.3089
E_1 (mm/rad)	0.0000	+942.141
E_2 (mm/rad^2)	0.0000	−851.776
E_3 (mm/rad^3)	0.0000	−636.897

TABLE 4. Complex ease-off. Basic settings $\mathbf{x}_0$ and corrections $\mathbf{s}$ obtained by the (complete) SVD.

PARAMETER	BASIC VALUE $\mathbf{x}_0$	SOLUTION $\mathbf{x}_6$
Cutter point radius R_p (mm)	79.0130	79.0311
Spherical radius R_1 (mm)	350.8970	736.434
Blade angle α_p (deg)	17.4200	17.9601
Radial setting S_0 (mm)	72.1400	72.1419
Blank offset E_0 (mm)	−5.0800	−5.07302
Sliding base B_0 (mm)	−1.5192	−1.57686
Cradle angle q_0 (deg)	59.7369	59.7859
Machine root angle γ_0 (deg)	33.6731	33.6573
Ratio of roll m_0	1.7066	1.67457
2C	0.0226	0.506831
6D	−0.0329	-13.4053
24E	0.0000	34.0435
120F	0.0000	480.525
Mach. center to back D_0 (mm)	2.7184	2.74793
B_1 (mm/rad)	0.0000	−5.04039
B_2 (mm/rad^2)	0.0000	−20.6893
B_3 (mm/rad^3)	0.0000	2669.31
E_1 (mm/rad)	0.0000	3.44381
E_2 (mm/rad^2)	0.0000	−31.0423
E_3 (mm/rad^3)	0.0000	−1992.94

TABLE 5. Complex ease-off. Basic settings $\mathbf{x}_0$ and new setting $\mathbf{x}_6$ obtained by the Levenberg-Marquardt algorithm.

ACKNOWLEDGMENTS

The support of *Avio S.p.A.* is gratefully acknowledged.

REFERENCES

[1] Krenzer, T. J., and Knebel, R., 1983. "Computer aided inspection of bevel and hypoid gears". *SAE Paper 831266*.

[2] Krenzer, T. J., 1984. "Computer aided corrective machine settings for manufacturing bevel and hypoid gear sets". *AGMA Paper 84FTM4*.

[3] Litvin, F. L., Kuan, C., Wang, J., Handschuh, R., Masseth, J., and Maruyama, N., 1993. "Minimization of deviations of gear real tooth surfaces by coordinate measurements". *ASME Journal of Mechanical Design,* ***115***, pp. 995–1001.

[4] Visual Numerics, I., 2006. *IMSL Fortran Numerical Libraries - Version 6.0*. Visual Numerics, Houston.
[5] Lin, C.-Y., Tsay, C.-B., and Fong, Z.-H., 1998. "Computer-aided manufacturing of spiral bevel and hypoid gears with minimum surface deviation". *Mechanism and Machine Theory,* ***33***, pp. 785–803.
[6] Shih, Y.-P., and Fong, Z.-H., 2007. "Flank modification methodology for face-hobbing hypoid gears based on ease-off topography". *Journal of Mechanical Design,* ***129***, pp. 1294–1302.
[7] Shih, Y.-P., and Fong, Z.-H., 2008. "Flank correction for spiral bevel and hypoid gears on a six-axis CNC hypoid generator". *Journal of Mechanical Design,* ***130***, p. 062604.
[8] Shih, Y.-P., 2010. "A novel ease-off flank modification methodology for spiral bevel and hypoid gears". *Mechanism and Machine Theory,* ***45***(8), pp. 1108 – 1124.
[9] Gabiccini, M., Artoni, A., Di Puccio, F., and Guiggiani, M., Besançon, June, 2007. "A regularization method for hypoid gear synthesis using the invariant approach". In 12th IFToMM World Congress 2007, IFToMM.
[10] Hansen, P. C., 1997. *Rank-deficient and discrete ill-posed problems. Numerical aspects of linear inversion*. SIAM, Philadelphia.
[11] Gosselin, C., Nonaka, T., Shiono, Y., Kubo, A., and Tatsuno, T., 1998. "Identification of the machine settings of real hypoid gear tooth surface". *ASME Journal of Mechanical Design,* ***120***, pp. 429–440.
[12] Fan, Q., DaFoe, R., and Swanger, J., 2008. "Higher-order tooth flank form error correction for face-milled spiral bevel and hypoid gears". *Journal of Mechanical Design,* ***130***, p. 072601.
[13] Fan, Q., 2010. "Tooth surface error correction for face-hobbed hypoid gears". *Journal of Mechanical Design,* ***132***, p. 011004.
[14] Litvin, F. L., Zhang, Y., Kieffer, J., and Handschuh, R. F., 1991. "Identification and minimization of deviations of real gear tooth surfaces". *ASME Journal of Mechanical Design,* ***113***, pp. 55–62.
[15] Lin, C.-Y., Tsay, C.-B., and Fong, Z.-H., 2001. "Computer-aided manufacturing of spiral bevel and hypoid gears by applying optimization techniques". *Journal of Materials Processing Technology,* ***114***, pp. 22–35.
[16] Artoni, A., Gabiccini, M., and Guiggiani, M., 2008. "Non-linear identification of machine settings for flank form modifications in hypoid gears". *Journal of Mechanical Design,* ***130***, p. 112602.
[17] Argyris, J., Fuentes, A., and Litvin, F., 2002. "Computerized integrated approach for design and stress analysis of spiral bevel gears". *Computer Methods in Applied Mechanics and Engineering,* ***191***, pp. 1057–1095.
[18] Fong, Z.-H., 2000. "Mathematical model of universal generator with supplemental kinematic flank correction motions". *ASME Journal of Mechanical Design,* ***122***, pp. 136–142.
[19] Hutschenreiter, U., 1996. "A new method for bevel gear tooth flank computation". *Computational Differentiation - Techniques, Applications and Tools*, pp. 329–341.
[20] Gleason Corporation, 2011. Computer Aided Gear Engineering (*CAGE*^{TM}). http://www.gleason.com/b_software_cage.html, Accessed 14 February.
[21] Thomas, J., and Vogel, O., 2005. "6M machine kinematics for bevel and hypoid gears". *VDI - Berichte Nr. 1904,* ***1***, pp. 435–451.
[22] Litvin, F. L., and Fuentes, A., 2004. *Gear Geometry and Applied Theory*. PTR Prentice Hall, Englewood Cliffs.
[23] Gabiccini, M., 2009. "A twist exponential approach to gear generation with general spatial motions". *Mechanism and Machine Theory,* ***44***(2), pp. 382–400.
[24] Nocedal, J., and Wright, S. J., 1999. *Numerical Optimization*. Springer Verlag, New York.
[25] Strang, G., 1986. *Linear Algebra and Its Applications*, third ed. Harcourt Brace Jovanovich Publishers, San Diego.
[26] Fan, Q., and Dafoe, R. S., 2005. "Development of bevel gear face hobbing simulation and software". *VDI - Berichte Nr. 1904,* ***1***, pp. 485–504.
[27] Conn, A. R., Gould, N. I. M., and Toint, P. L., 2000. *Trust-region methods*. SIAM, Philadelphia.
[28] Stadtfeld, H. J., 1993. *Handbook of Bevel and Hypoid Gears*. Rochester Institute of Technology, Rochester.